Available online at www.sciencedirect.com
SCIENCE DIRECT®
Precambrian Research 131 (2004) 1–21
Precambrian Research
www.elsevier.com/locate/precamres

C–O–Sr isotopic stratigraphy of cap carbonates overlying Marinoan-age glacial diamictites in the Paraguay Belt, Brazil

Carlos J.S. de Alvarenga*, Roberto V. Santos, Elton L. Dantas

Instituto de Geociências, Universidade de Brasília, Campus Universitário, Asa Norte, CEP:70910-900, Brasília, DF, Brazil

Received 25 January 2002; accepted 2 December 2003

Abstract

The Neoproterozoic Paraguay Belt, located along the southeastern border of the Amazon Craton and eastern border of the Rio Apa Block, comprises a thick passive margin succession of glaciomarine turbidites, carbonates and siliciclastic sedimentary rocks that were deformed during the Brasiliano/Pan-African Orogeny. The carbonate sequence comprises a 1300 m thick succession of platformal carbonate rocks (Araras Formation), which directly overlie Marinoan glacial diamictites (Puga Formation). The late Neoproterozoic age of this carbonate sequence is indicated by the presence of *Cloudina lucianoi* and *Corumbela werneri* found in the upper part of the Corumbá Group (Southern Paraguay Belt).

Carbon and Sr isotope data were obtained on marine carbonate samples across three different sections of the Araras Formation. $\delta^{13}C_{PDB}$ values of the carbonate from the border of the basin range between −10.5 and −2.7‰, including a short stratigraphic interval of cap dolomite (22 m) directly overlying diamictites. The isotopic profile across the basal 200 m of deep shelf laminated microcrystalline limestone and clay-limestone (cap-carbonate), that overlie glacial diamictites, also show negative $\delta^{13}C_{PDB}$ values (−5.3 and +0.6‰). In contrast with the lower portion of the carbonate sequence, a 800 m thick unit of shallow-water dolostones forming the upper part of the carbonate sequence present uniform positive $\delta^{13}C_{PDB}$ values ranging from +1.9 to +2.4‰. Dolostone and arenaceous dolostone of the upper parts of the Araras Formation have high $\delta^{13}C_{PDB}$ values (+4.1 to +9.6‰) which are followed by an abrupt decrease in $\delta^{13}C$ values, down to −1.0‰.

The carbon isotope profile of the Paraguay Belt is quite different from the Bambuí Group an other important Neoproterozoic sequences in Central Brazil, which also overlie glacial sediments. Negative $\delta^{13}C_{PDB}$ values are found only within the lowermost meters of these sequence and are followed by an important and extensive positive carbon isotope excursion (values ranging from +6.9 to +16.0‰). On the other hand, the $\delta^{13}C_{PDB}$ profile observed across the Araras Formation exhibits an approximately 200 m thick section of carbonates with low $\delta^{13}C_{PDB}$ values.

Carbonates of the Araras Formation have $^{87}Sr/^{86}Sr$ ratios ranging from 0.70753 to 0.70803, comparable to cap carbonates that overly Marinoan glacial deposits from other neoproterozoic sequences.

Keywords: Cap carbonate; Carbon isotope; Glaciation; Neoproterozoic; Sr isotope; Stratigraphy

1. Introduction

Glacial events are well documented in the Cryogenian (850–650) and Neoproterozoic III (650–540) periods. The older glacial event is generally termed Sturtian-Rapitan (from ∼760 to 700 My), and the younger is referred to as the Varanger or Marinoan (from ∼620 to 580 My) (Young, 1995; Hoffman et al., 1998a; Kennedy et al., 1998; Saylor et al., 1998; Brasier et al., 2000; Walter et al., 2000; Hyde et al., 2000). Both glacial events, which appear to

* Corresponding author. Fax: +55-61-307-2436.
E-mail address: alva1@unb.br (C.J.S. de Alvarenga).

0301-9268/$ – see front matter © 2004 Elsevier B.V. All rights reserved.
doi:10.1016/j.precamres.2003.12.006

have reached very low latitudes (Hoffman et al., 1998a; Kennedy et al., 1998; Hyde et al., 2000; Jacobsen, 2001; Kennedy et al., 2001), have been identified in central Brazil and are both overlain by cap carbonate. The older cap carbonate sequence covers large areas in the São Francisco Craton and also occurs in the surrounding Neoproterozoic folded belts (Rio Preto, Araçuaí, Ribeira and Brasília). Cap carbonate within this sequence are found at the base of the Bambuí and Una groups, which overlie respectively glacial diamictites of the Jequitaí and Bebedouro formations (Dardenne, 1978; Karfunkel and Hoppe, 1988; Misi and Kyle, 1994; Misi and Veizer, 1998; Uhlein et al., 1999; Santos et al., 2000). These diamictites were dated between 700 and 800 Ma (Toulkerids et al., 1999; Santos et al., 2000) and were, therefore, related to the "Sturtian" event. The younger carbonate sequence is described

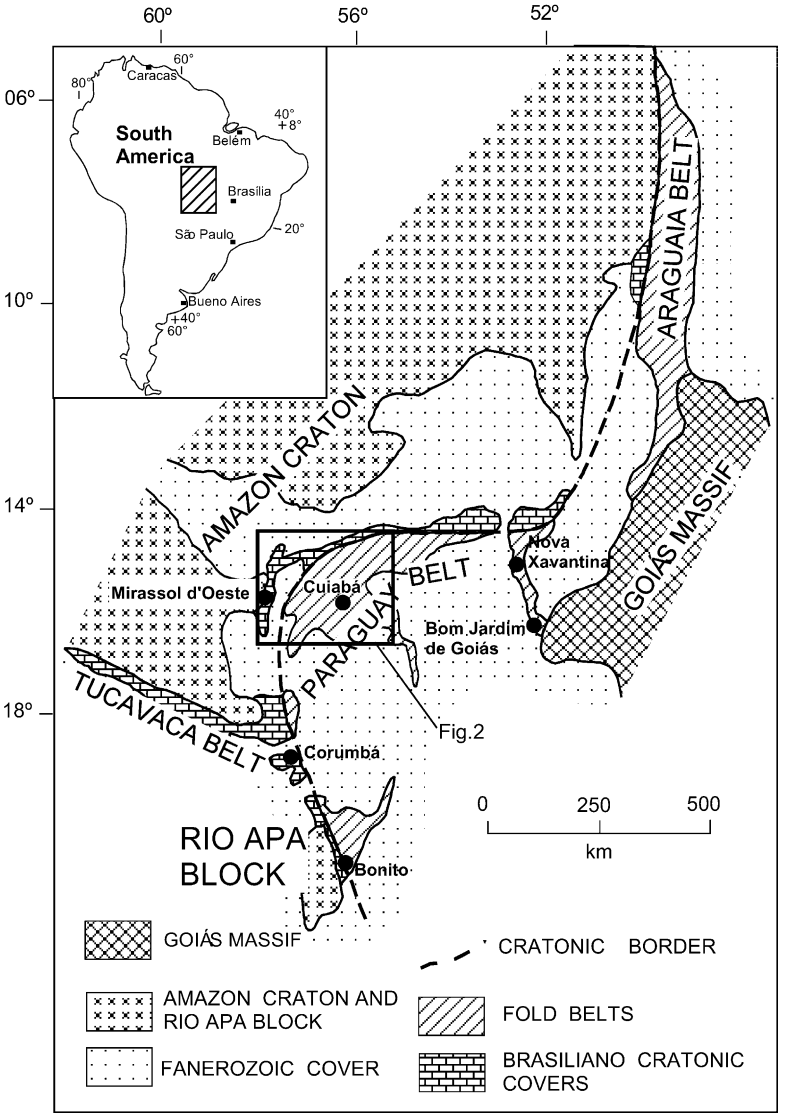

Fig. 1. Geological map of the Brasiliano Paraguay Belt along the border of the Amazon Craton and the Rio Apa Block. According to Scobbenhaus et al. (1981), Litherland et al. (1986), de Alvarenga and Trompette (1993) and Trompette (1994). The inset square indicates the location of Fig. 2.

in the Paraguay Belt and post-dates the late Neoproterozoic Marinoan glacial sediments (de Alvarenga and Trompette, 1992; Trompette, 1994). This glacial event has been discussed in many stratigraphic, tectonics and paleogeography studies concerning Gondwana and Laurentia supercontinents models (Schimidt et al., 1991; Trompette, 1996; Kennedy et al., 1998; Myrow and Kaufman, 1999; Condon and Prave, 2000).

In the Paraguay Belt the glacial event was recorded as a glaciomarine depositional system (Puga Formation) forming a large platform at the border of the basin, and as a glacial derived turbidite deposits (Cuiabá Group) that occur in the slope and outer slope parts of the basin (de Alvarenga and Trompette, 1992). Near the city of Corumbá (Fig. 1) this glaciomarine sequence is overlain by a carbonate sequence, containing Ediacara-like fauna (Vendian) in its upper part (Tamengo Formation). The microfossil assemblage is dominated by syphozoar *Corumbella werneri* (Hahn et al., 1982; Walde et al., 1982), *Babvinella faveolata*, *Vandalosphaeridium* sp., *Cloudina lucianoi* (Zaine and Fairchild, 1985, 1987), *Soldadophycus bossii*, *Titanotheca* and the vendotaenid *Eoholynia corumbensis* sp. (Gaucher et al., 2003). The presence of these fossils suggests that the carbonate sequence was deposited during the upper-Vendian (590–545 Ma) (Zaine and Fairchild, 1985, 1987; Zaine, 1991; de Alvarenga and Trompette, 1992; Trompette, 1996, 1997; Trompette et al., 1998; de Alvarenga et al., 2000; Gaucher et al., 2003).

Carbon-isotope and $^{87}Sr/^{86}Sr$ stratigraphy have been widely used to correlate cap carbonate strata overlying Sturtian and Marinoan glaciogenic rocks worldwide (e.g., Kaufman and Knoll, 1995; Knoll et al., 1995; Kaufman et al., 1997; Kennedy et al., 1998; Walter et al., 2000). Most isotope stratigraphic data for Neoproterozoic limestones in South America are related to post-Sturtian carbonate rocks from the São Francisco Basin (Bambuí and Una groups) (Chang et al., 1993; Iyer et al., 1995; Misi and Veizer, 1998; Martins, 1999; Santos et al., 2000), as well as to carbonates of the Araras Formation and Corumbá Group, for which very preliminary $\delta^{13}C_{PDB}$ and $^{87}Sr/^{86}Sr$ data are available (Zaine, 1991; Boggiani et al., 1997; Gaucher et al., 2003).

In this paper we present new C-isotope, Sr-isotope and chemical data for profiles across limestones of post-Marinoan Neoproterozoic glacial rocks of the Araras Formation, northern Paraguay Belt. This unit consists of an approximately 1300 m thick well-preserved section of limestones and dolostones, which are part of one of the most extensive Neoproterozoic sequences in central South America. Due to the absence of fossils and geochronological data, the carbon and Sr isotope profiles presented here may be used to correlate these rocks with similar Neoproterozoic sequences from other parts of the world.

2. Geological setting

The Paraguay Belt is located along the southeastern border of the Amazon Craton and eastern border of Rio Apa Block (Fig. 1). It comprises a thick succession of glaciomarine, turbidite, carbonate and siliciclastic sedimentary rocks deposited in a passive margin environment (de Alvarenga, 1990; de Alvarenga and Saes, 1992; de Alvarenga and Trompette, 1992, 1993; de Alvarenga et al., 2000). In the Paraguay Belt these rocks have been affected by a young Brasiliano-Pan African Orogeny, around the Early-Middle Cambrian boundary (Trompette, 1994, 1997; Pimentel et al., 1996; de Alvarenga et al., 2000), followed immediately by post-orogenic sub-alkaline granite magmatism at ca. 500 Ma (de Almeida and Mantovani, 1975). Deformation and metamorphism increase from weak effects along the western border of the basin to low-grade metamorphism in the inner parts of Paraguay Belt (de Alvarenga and Trompette, 1993) (Figs. 2 and 3).

The northern Paraguay Belt presents four major lithostratigraphic units that exhibit lateral facies variations, mainly between the western border and the central eastern portion of the basin. Exposure of organic-rich shales and limestones of the lower unit are limited to cores of anticline structures near Poconé (Fig. 2). Overlying these rocks are glaciomarine and turbiditic sediments which are followed by a carbonate sequence. The contact between these two lithostratigraphic units corresponds to the end of the glacial event in the basin and defines a stratigraphic marker related to sea-level rise. The uppermost unit comprises a succession of siliciclastic rocks including sandstone, mudstone and arkose.

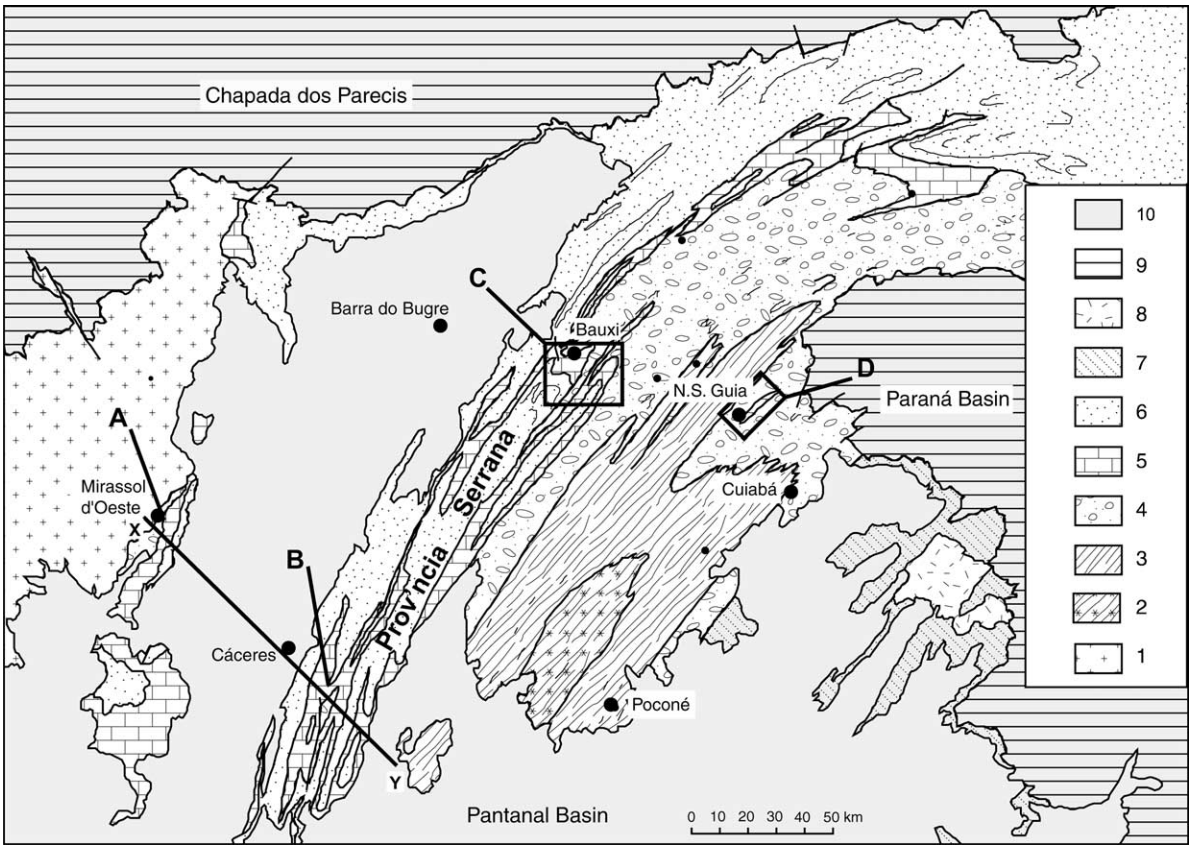

Fig. 2. Geological map of part of the Paraguay Belt (after de Alvarenga, 1990; de Alvarenga and Trompette, 1993). Localities studied are: (A) Mirassol d'Oeste (MDO); (B) Província Serrana Cárceres area (PS); (C) Província Serrana Bauxi area (PS); and (D) Nossa Senhora da Guia syncline (NSG). *X–Y* is location of the cross section shown in Fig. 3. (1) Amazon Craton, (2) lowest unit: phyllite, graphite-phyllite, quartzite and dolomite, (3) glacially influenced unit: turbidites of the Cuiabá Group, (4) glacially influenced unit: diamictite associations and glaciogenic deposits (Cuiabá Group, Puga Formations), (5) carbonate unit: limestones and dolostones of the Araras Formation and Guia Facies, (6) upper siliciclastic unit: sandstones, arkoses, siltstones and shales (Raizama and Diamamtino formations), (7) fine-grained turbidites and phyllites (southeast of Cuiabá Group), (8) São Vicente Granite (500 Ma), (9) Paleozoic-Mesozoic of the Paraná and Parecis basins, (10) Cenozoic (Pantanal Basin).

2.1. Stratigraphic units

The stratigraphy of the Paraguay Belt was investigated along regional geological cross sections across the southwestern border of the Amazon Craton (Figs. 1–3) (de Alvarenga and Saes, 1992; de Alvarenga and Trompette, 1992, 1993).

The lowest unit is a sequence of phyllite, quartzite, graphite phyllite and magnesian marble. These low-grade rocks are folded and display penetrative crenulation cleavage developed mainly in the phyllites.

The Glacially influenced unit occurs both on the cratonic area (Puga Formation) as well as in the fold belt (Cuiabá Group). Glaciogenic and turbiditic sediments are identified along the transitional zone between the Amazon Craton, to the northwest, and the Paraguay Belt, to the southeast (de Alvarenga and Trompette, 1992). The glacial origin of the diamictites in the Paraguay Belt was first recognized by Maciel (1959). Subsequently these diamictites have been re-examined and described as a glacial sequence composed of diamictite and associated conglomerate, sandstone and shale (de Almeida, 1964a,b;

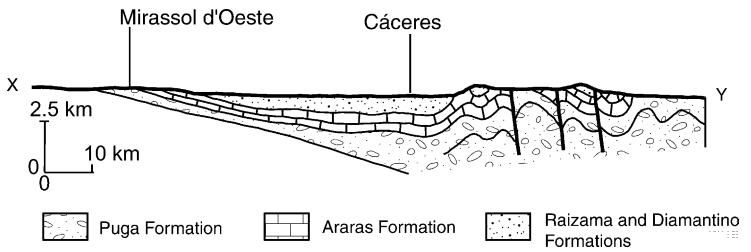

Fig. 3. *X–Y* geological section of the border of the Amazon Craton and into the Paraguay Belt (see Fig. 2 for location). Deformation increases from weak effects in the MDO region to southeastern folded rocks in the PS region.

Rocha-Campos and Hasuí, 1981). Clasts of the diamictites are derived mostly from the basement and include granite, gneiss, quartzite, quartz and schist, as well as abundant detrital mica. The diamictites also present a reddish to greenish clay-rich matrix as well as striated clasts.

The sedimentation model proposed for the glacially influenced unit includes three main depositional systems: platformal, slope and outer slope (de Alvarenga and Trompette, 1992). Glaciomarine sediments which cover the Amazon Craton on the western inner shelf, were partially reworked by gravity-flows on the eastern, outer shelf. The deposits of the inner shelf show an alternation of dominant massive diamictite (Fig. 4), sandstone and fine-grained sediment with few dropstones. In the outer shelf, the massive diamictites are progressively replaced by an association of massive diamictites, stratified diamictites and fine-grained sediments. The slope depositional system is characterized by glaciomarine derived sediments that were reworked by powerful gravity flows. This process resulted in the down-slope accumulation of conglomerates, sandstones and diamictites, along a submarine channel systems. Deposition on the outer slope was dominated by fine-grained deposits (phyllite and metasiltstone) related to turbidite cycles, in which direct glacial influence is restricted to the presence of a few isolated clasts or dropstones (Fig. 5).

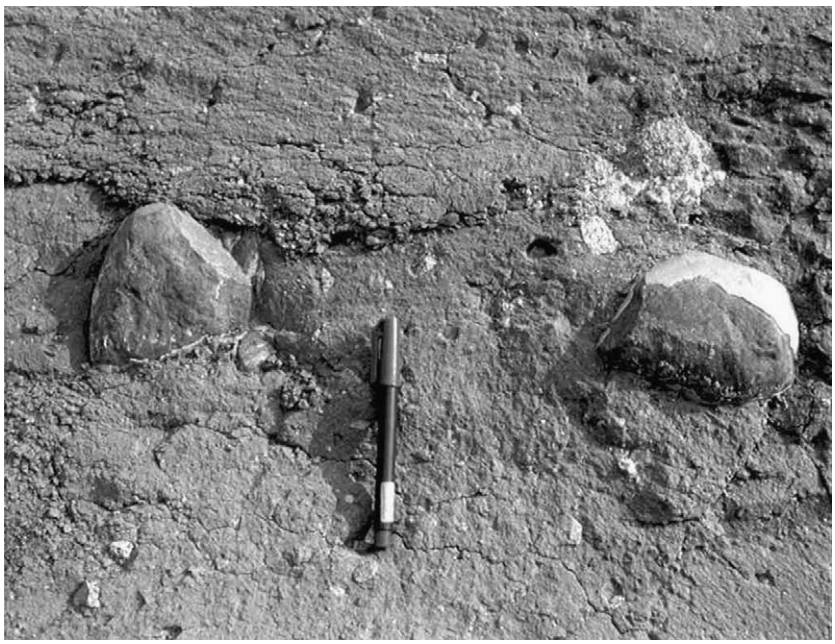

Fig. 4. Massive diamictites with large clasts of quartzite. Other small clasts are granite, gneiss, quartz, schist and abundant detrital mica.

Fig. 5. Laminated fine-grained sediments dominated by turbidity process. The evidence of glacial influence is represented by a few dropstones within laminated sediments.

The Carbonate Unit overlies the glaciogenic unit and marks the end of the glacial event in the basin. The Araras Formation consists of approximately 1200 m of limestones and dolostones (Luz and Abreu Filho, 1978). In the Província Serrana region (PS) these limestone beds are finely stratified in the lower 200 m and grade upwards to dolograinstone and doloosparite/doloosparudite rocks (de Alvarenga et al., 2000). To the east, the carbonate unit gives place to a thick carbonate sequence on the border of the craton and to a mud-rich limestone and laminated metasiltstone towards the central part of the belt, included in the Guia Facies of the Cuiabá Group.

The upper siliciclastic unit is known as the Alto Paraguay Group and consists of two siliciclastic formations; cross-bedded sandstone (fine- to very coarse-grained sub-arkose) at the base (Raizama Formation); and red shale, siltstone and arkose at the top (Diamantino Formation). The contact between these two units is transitional and marked by intercalation of sandstone, laminated mudstone, and siltstone. The thickness of these units were estimated to be approximately 2800 m (Barros et al., 1982). Shales of the lower part of the Diamantino Formation gave a Rb–Sr isochron age of 568 ± 20 Ma, interpreted as the age of diagenesis (Bonhomme et al., 1982; Cordani et al., 1985).

3. Studied sections

Carbonate rocks were systematically sampled along profiles across the northern part of the Paraguay Belt. These rocks grade from the inner shelf (near shore) shallow deposits of the Mirassol d'Oeste region (MDO), to the down-slope accumulation deposits of the Província Serrana region (PS), and to the outer-slope part of the basin, in the Nossa Senhora da Guia syncline (NSG) (Fig. 2). These rocks were deposited on an asymmetric basin that evolved as a continental passive margin platform and were partially affected by deformational processes and low-grade metamorphism. The three areas studied here display gradual increase on deformation and metamorphism from MDO-PS to NSG. Hence, MDO rocks were not deformed and metamorphosed, whereas PS rocks were folded, but not metamorphosed, and NSG rocks were folded and affected by very low-grade metamorphic conditions. In the next sections a brief description of the main geological features of the areas investigated is presented.

3.1. Mirassol d'Oeste (MDO)

The western border of the basin include diamictite and fine-grained sediment with few dropstones (Puga

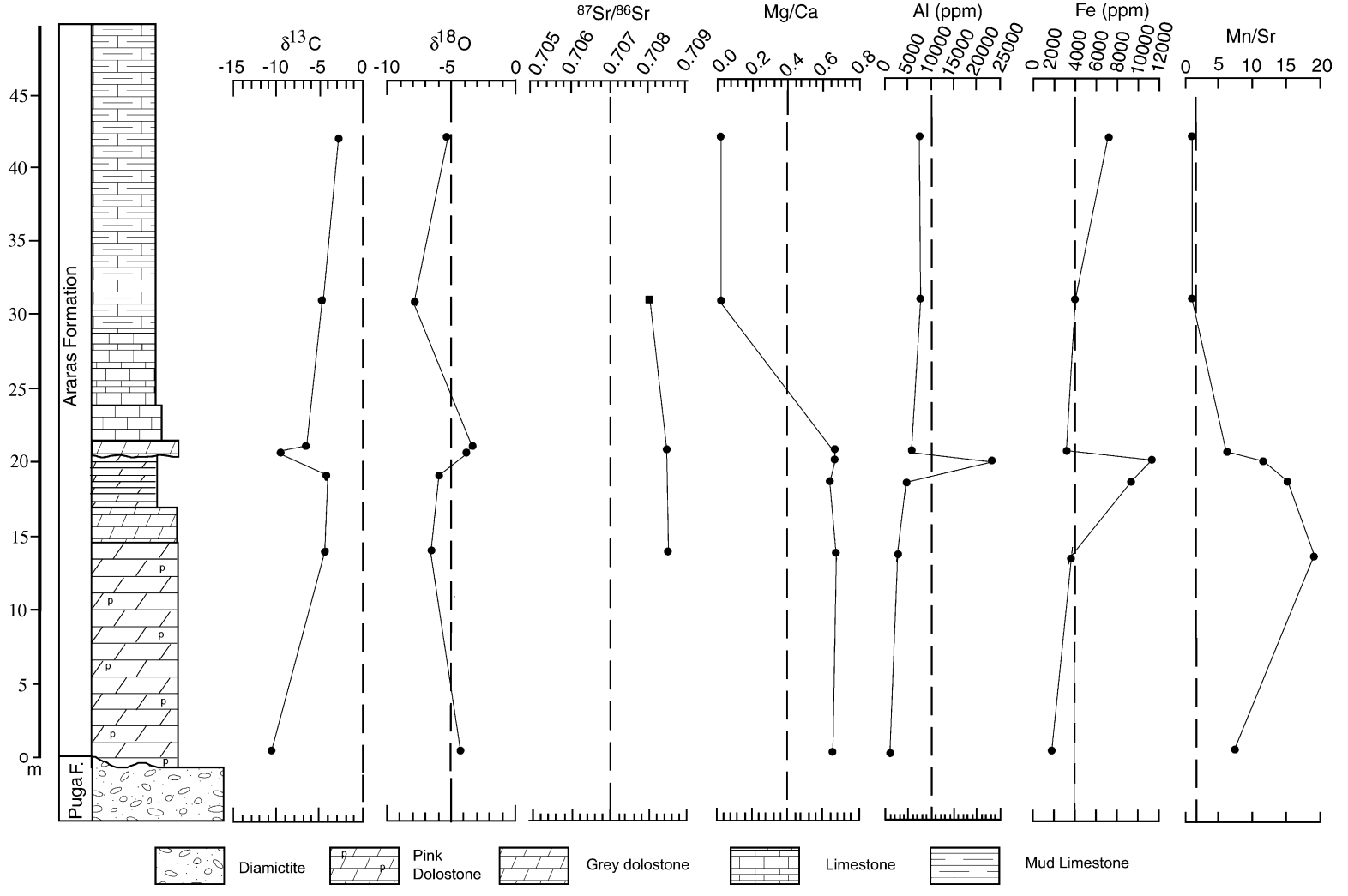

Fig. 6. Stratigraphic section and variations of $\delta^{13}C_{PDB}$, $\delta^{18}O_{PDB}$, $^{87}Sr/^{86}Sr$ and geochemical data of the cap dolostone overlying the glaciogenic Puga Formation in Mirassol d'Oeste. The square represents primary Sr isotope ratios.

Formation), as well as carbonate rocks (Araras Formations) which are poorly exposed (Figs. 2, 3, and 6). The Mirassol d'Oeste diamictite-pelite section is 100 m thick and overlies Paleo/Mesoproterozoic metamorphic rocks. This unit was described as a cratonic platformal facies made up of massive and stratified diamictite containing basement clasts, as well as of laminated silty mudstone (de Alvarenga and Trompette, 1992). The continuous cap carbonate sequence (Araras Formation) directly overlying the diamictites (Puga Formation) was sampled in a >45 m thick section of dolostone and limestones exposed in a mining quarry (Fig. 6). This section is made of a lower and an upper unit. The lower unit has 22 m thick of laminated and peloidal pink dolostones, which is followed by an upper irregular layer of sand-bearing dolostone (~0.8 m thick) (Fig. 6). Primary sedimentary structures, such as stromatolites and laminations, were partially obliterated by the dissolution and recrystallization (Fig. 7A). The first 15 m of pink dolostones directly blanketing the glacial diamictites also have centimetric voids, filled with hydrocarbon, calcite and dolomite (Fig. 7B), that are related to carbonate dissolution and chemical compactation (stylolites). The upper unit of the carbonate section is characterized by the intercalation of homogeneous and laminated fine-grained limestone and laminated mudstone suggesting eustatic sea level rise.

The carbonate sequence of Mirassol d'Oeste exhibits evidence of shallow water deposition (lower cap-dolostone), followed by a transgressive sequence of limestone. This interpretation is supported by the presence of gypsum and anhydride pseudomorphs in the Araras Formation limestones (Zaine, 1991).

3.2. Província Serrana (PS)

In the Província Serrana (PS) weakly metamorphosed limestone and dolostone are exposed in a sequence of synclines and anticlines (Figs. 2 and 3). Samples were collected across two profiles that include glacial derived sediments and carbonate rocks: one in the vicinities of Cáceres and the other in the Bauxi area (Fig. 2).

The *Glacially influenced unit* of the PS region consists of massive diamictite, stratified diamictite, massive sandstone and other fine-grained sediments (de Alvarenga and Trompette, 1992). In the Bauxi area this unit can be subdivided into three stratigraphic facies: (1) fine-grained sediments with local dropstones; (2) intercalation of sandstone, pebble-bearing sandstone, and diamictite; and (3) massive layers of diamictite (up to 40 m thick) intercalated with fine-grained rocks. Clasts in the diamictite and sandstone include mainly quartzite, sandstone, granite, basic volcanic rocks, rhyolite, and rare siltstone, mudstone and limestone.

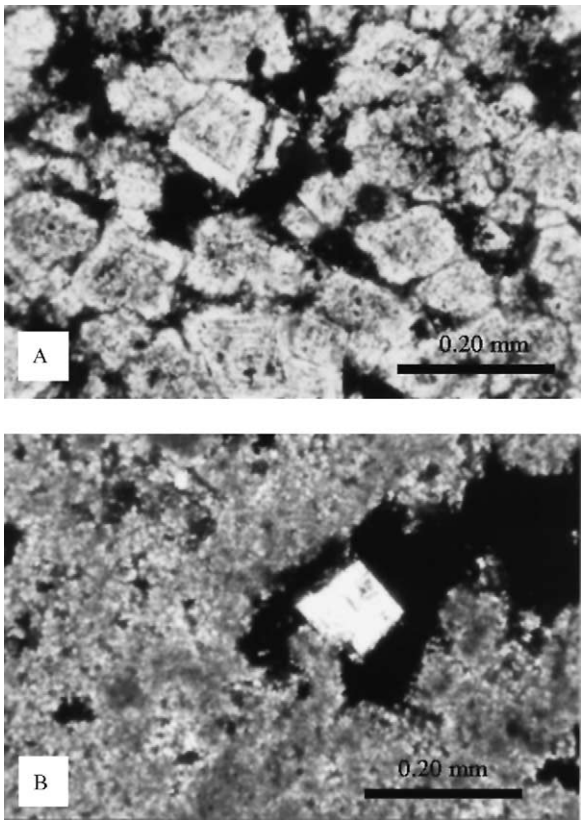

Fig. 7. Cap dolomite formation in Mirassol d'Oeste; thin section photomicrographs. (A) Recrystallization of dolomite rhombs (sample Mira 7). (B) Peloidal dolostones with small cavity structures filled with hydrocarbon and dolomite crystal.

The *carbonate unit* overlies the diamictite and marks the beginning of post-glacial transgression. This unit can be divided into a lower limestone facies and an upper dolostone facies (Fig. 8). The lower facies comprises 220 m of laminated mudstone -limestone and limestone (Fig. 9), with local laminated limestone slump deposits. In general, this carbonate facies presents decrease in the amount of mudstone laminae

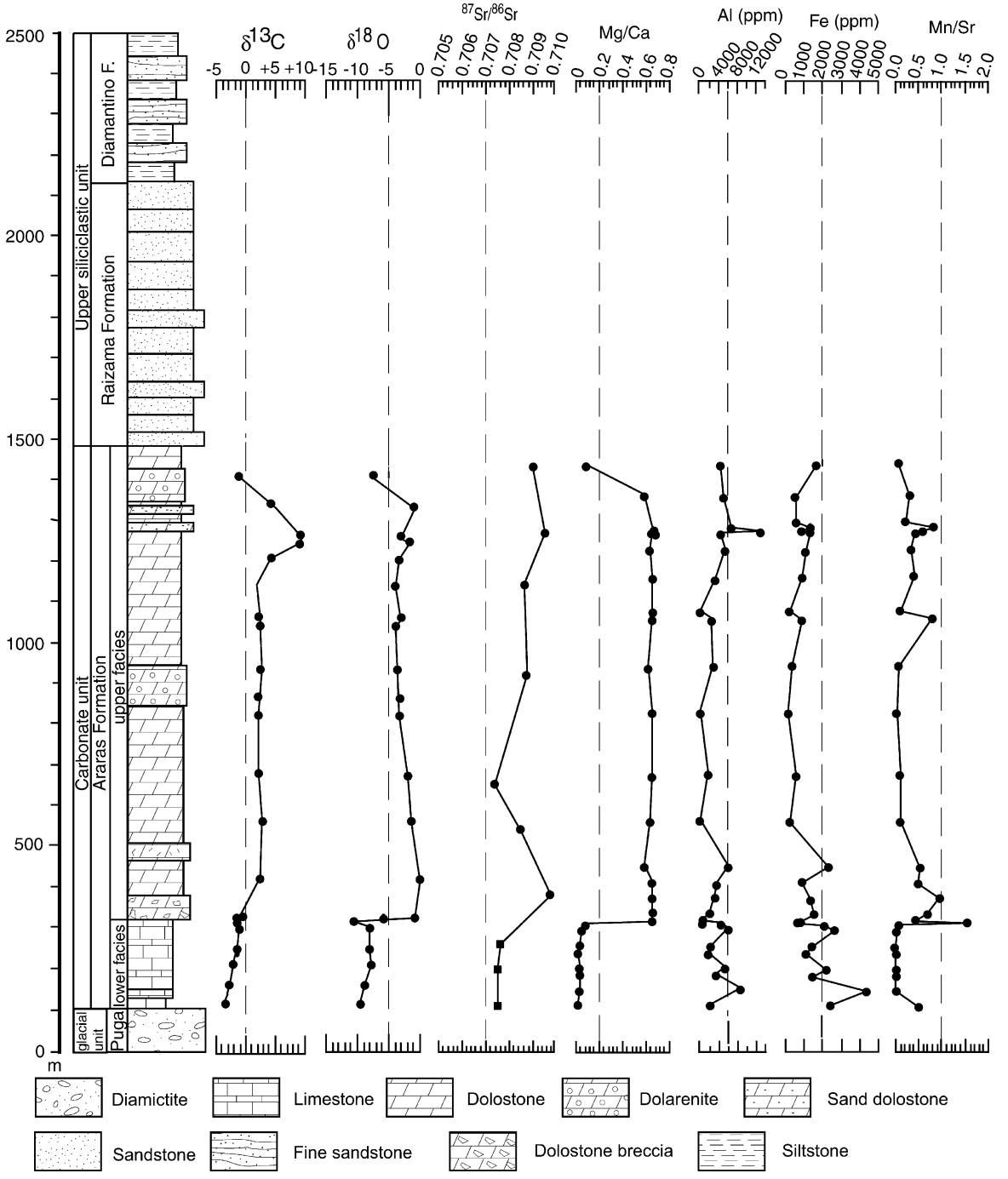

Fig. 8. Stratigraphic section and variations of $\delta^{13}C_{PDB}$, $\delta^{18}O_{PDB}$, $^{87}Sr/^{86}Sr$ and geochemical data of the Carbonate Unit in the Província Serrana area. Samples were collected from the lower facies (cap carbonate), near Cáceres (section B), and for the upper facies in the Bauxi region (section C). See Fig. 2 for location of sections. The square represents primary Sr isotope ratio.

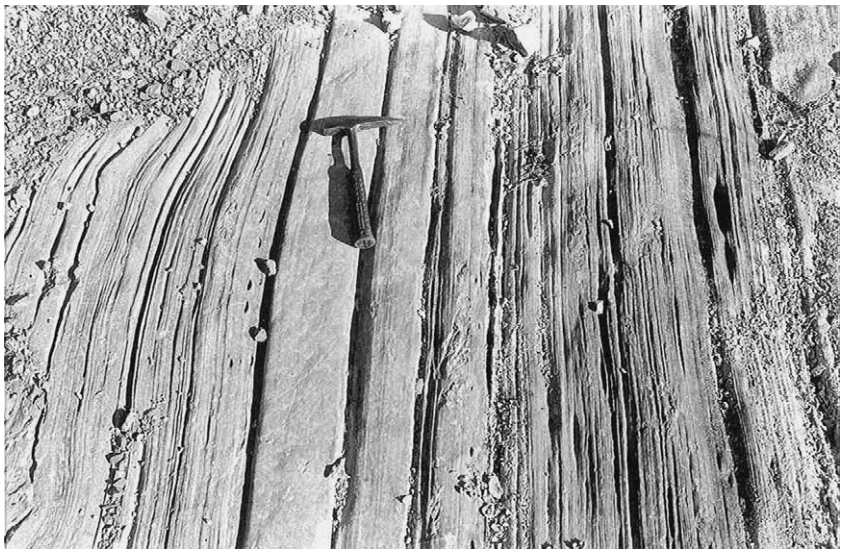

Fig. 9. Laminated limestones of the lower facies (cap carbonate) of the Araras Formation in the Província Serrana area (PS).

towards the top, suggesting shallowing of the water column.

The upper carbonate unit consists of more than 1100 m of shallow-shelf dolostone in which the presence of ooids and peloids indicates relatively high-energy environments. This dolostone facies outcrops along the Província Serrana Hills and overlie the laminated limestone. The lower part of the sequence consists of dolostone and dolostone breccia (clasts up to 1 m) in sharp contact with the underlying laminated limestone. They grade upwards to a sequence marked by the intercalation of laminated dolostones with 2–4 m thick beds of breccia (clasts up to 10 cm) and wackestone. Towards the top of

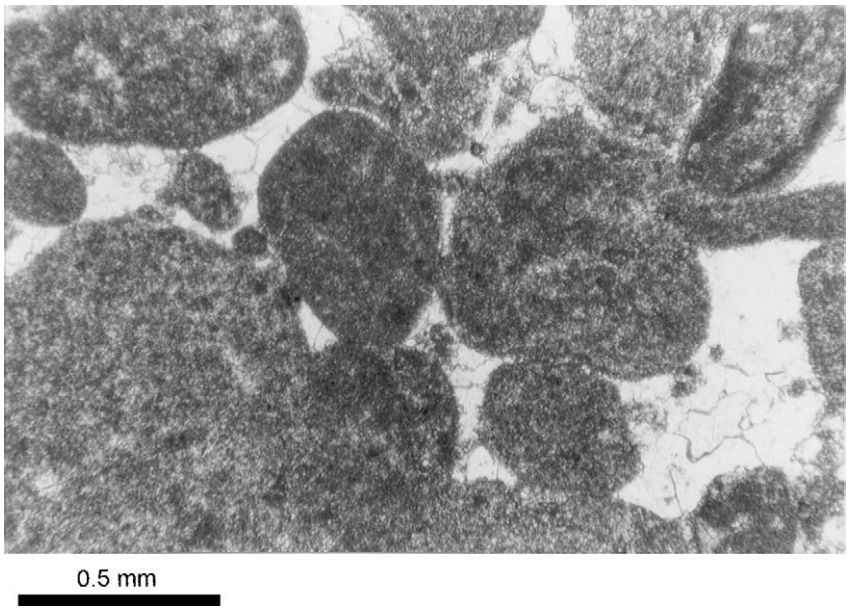

Fig. 10. Thin section photomicrographs of dolomitized oolite-intraclast grainstone that still preserve the original texture.

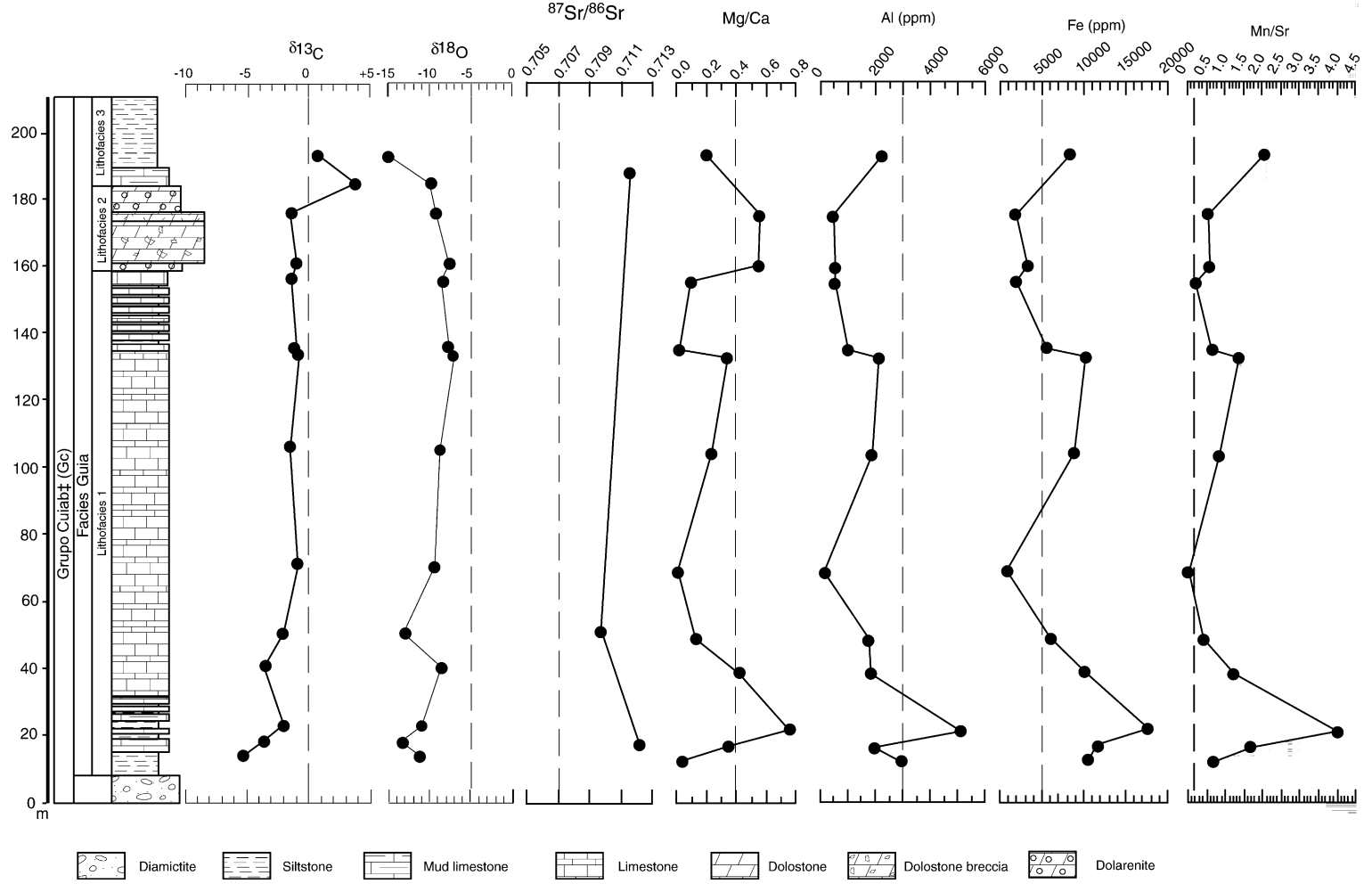

Fig. 11. Stratigraphic section and variations of $\delta^{13}C_{PDB}$, $\delta^{18}O_{PDB}$, $^{87}Sr/^{86}Sr$ and geochemical data of Carbonate Unit in the Nossa Senhora da Guia (NSG) section. Lithofacies 1: Interbedded limestones and black-gray siltstone, Lithofacies 2: Light gray oolitic and intraclastic dolostone (dolorudite and breccia—Fig. 12), Lithofacies 3: Limestones grading to shale siltstone.

the upper carbonate unit, the dolomite facies exhibits packstones and grainstones that are characterized by dolarenites and dolorudites (ooids, intraclasts) with sparse quartz and feldspar clasts (Fig. 10). Feldspatic sandstone beds cemented with dolomite (up to 2 m thick) and found in the upper parts of this sequence (Fig. 8) are interpreted as sediments deposited in a shelf environment that became shallower towards the top. For instance, while the lower portion of the upper facies is characterized by breccias related to storms waves and currents, the upper part of the sequence is characterized by shoals.

3.3. Nossa Senhora da Guia (NSG) syncline

The Nossa Senhora da Guia (NSG) area is located 30 km NW of Cuiabá and consists of an asymmetric syncline with the axis in the NE–SW direction (Fig. 1). The lower part of the sequence comprises glacial derived rocks characterized by massive diamictite with an abundant clay-silt matrix (up to 70%) and millimetric to centimetric clasts. These rocks are overlain by intercalations of shale and limestone that grade to siltstone and shale towards the top of the sequence. On a regional scale, these beds are interpreted as deposited in a deep zone of the platform.

The Carbonate Unit can be subdivided into three distinct lithofacies associations (Fig. 11). Lithofacies association 1 consists of ~140 m thick cyclic centimeter-scale beds of limestone with intercalation of black-gray siltstone and calcium carbonate. The limestone allochens are composed of ooids, peloids and intraclasts, generally less than 0.125 mm in diameter and composed of micrite and laminated calcilutite. The calcarenite reveals repeated successions of sedimentary structures including erosional bases, graded-bedding, rippled intervals and hummocky cross-stratification, indicating that they were deposited in a deep-water storm environment. Some of

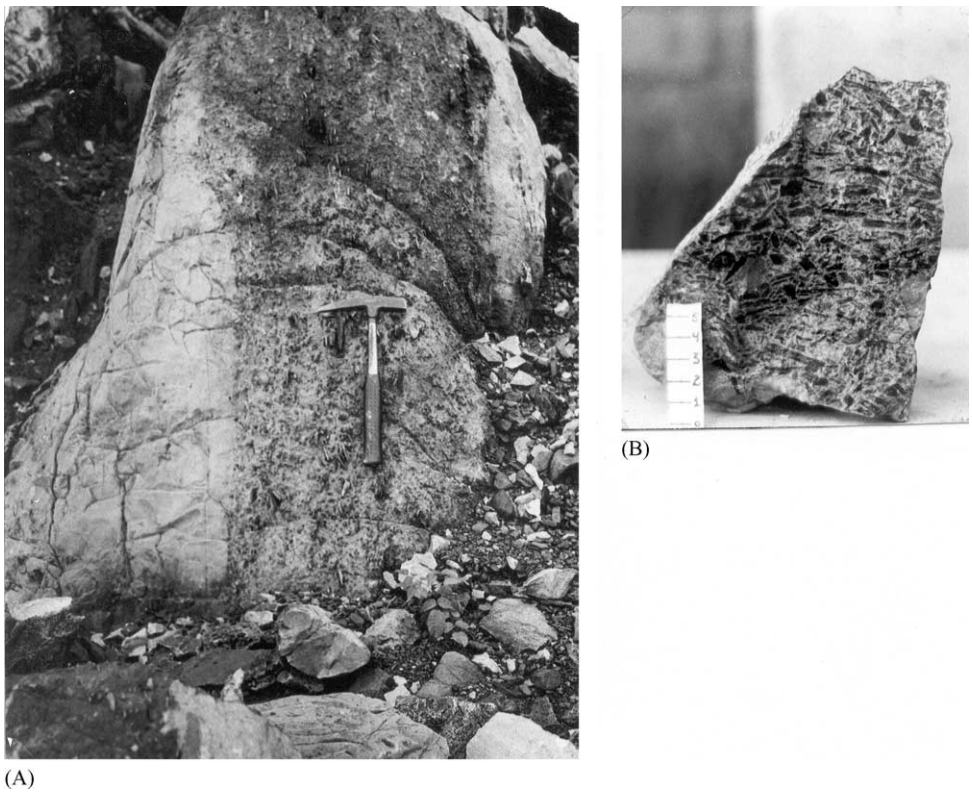

(A) (B)

Fig. 12. (A) Dolostone breccia layer in dolarenite of lithofacies 2 (where the hammer is located), from Guia Facies. (B) Detail of the dolostone breccia, tabular clasts are oriented subparallel to each other.

these limestone are fetid and rich in pyrite, suggesting anoxic conditions.

Lithofacies association 2 is characterized by an approximately 12 m thick light gray oolitic and intraclastic dolostone (dolorudite and breccia) (Fig. 12). Deposition of these sediments was affected by storms, thus suggesting shallow environment conditions.

Lithofacies association 3 consists of gray limestone beds and subordinate 5–15 cm thick beds of calcarenite. It also presents liquidization and slumping sedimentary structures, indicating high rates of sedimentation. Towards the top of the sequence the limestones grade to shale siltstones that were deposited in a deep-water environment.

4. Sampling and analytical methods

Forty-nine samples of lime carbonate and dolo carbonate rocks were collected at intervals from 5 to 40 m along profiles across the MDO, PS and NSG areas. MDO and PS presented no evidence of metamorphism, while NSG rocks were metamorphosed under low-grade metamorphic conditions.

Carbon and oxygen isotopic ratios of carbonates were obtained after reacting the samples with 100% H_3PO_4 at 25 °C for at least 12 h for calcite and for over 3 days for dolomite (McCrea, 1950). Samples and acid were pre-evacuated in a vacuum line before reaction, after which the evolving CO_2 was separated and analyzed for $\delta^{13}C_{PDB}$ and $\delta^{18}O_{PDB}$ using a Finnigan Delta E gas source mass spectrometer at the University of Brasília. The CO_2 oxygen isotope compositions were corrected to calcite and dolomite by applying, respectively, the fractionation factors 1.01025 and 1.01111. The uncertainties of the isotope measurements were 0.2‰ during the period of analyses.

For the $^{87}Sr/^{86}Sr$ analysis, 50 mg of carbonate powder samples were weighed into Teflon beakers and digested in weak acetic acid to dissolve only the carbonate fraction and avoid leaching of radiogenic ^{87}Sr and Rb from the non-carbonate constituents of the samples. Chemical procedures described by Derry et al. (1989), Asmeron et al. (1991), and Kaufman et al. (1993) were used. $^{87}Sr/^{86}Sr$ ratios were determined using a Finningan MAT 262 thermal ionization mass spectrometer in static mode at the geochronology laboratory of the University of Brasília. Analyses of NBS 987 standard carried out during the course of this work yield an average value of 0.710230 ± 8 (1σ). Uncertainties in individual analyses are better than 0.01% (2σ).

Samples for chemical analysis were weighted into Teflon beakers and attached with a HNO_3 and HF solution. The mixture was dried and attached again with HNO_3 and HF. After drying again all the solution, the residue was dissolved with HNO_3 and the resulting solutions was used to determine the elements Sr and Rb by ICP-MS, and Ca, Mg, Fe and Mn by ICP-AES.

5. Chemostratigraphy

The chemical composition of the samples were used mainly to evaluate the extend of post-depositional alteration, based on their Mn/Sr and Fe/Sr ratios and Sr content. The degree to which the carbonate rock samples were affected by post-depositional modifications is particularly important to evaluate whether they record the Neoproterozoic seawater isotopic composition. Carbon, oxygen and strontium isotope, as well as Ca, Mg, Mn, Fe, Al and Sr data for the profiles (MSD, PS and NSG) are in Tables 1–3.

Table 1
Carbon, oxygen, Sr isotopes and elemental composition of samples from the MDO profile (Nd = not determined)

Sample	Lithology	Height (m)	$\delta^{13}C_{PDB}$	$\delta^{18}O_{PDB}$	Mg/Ca	Al (ppm)	Fe (ppm)	Mn (ppm)	Sr (ppm)	Fe/Sr	Mn/Sr	$^{87}Sr/^{86}Sr$
Mira-15	Dolostone	0	−10.5	−4.3	673.6	612	1488	422	52	28.6	8.1	Nd
Mira-01	Dolostone	4	−4.3	−6.6	617.3	2250	3167	1345	74	42.8	18.2	0.70852
Mira-04	Dolostone	9	−4.1	−6.0	600.0	4768	10440	1264	69	151.3	18.3	Nd
Mira-07	Sand-dolostone	10.5	−9.6	−3,8	617.1	23503	12511	764	56	223.4	13.6	Nd
Mira-06	Dolostone	11	−7.0	−3.4	611.5	6263	3899	411	56	69.6	7.3	0.70848
Mira-09	Limestone	21	−4.6	−7.9	21.0	7631	4449	459	412	10.8	1.1	0.70803
Mira-12	Limestone	32	−2.7	−5.3	21.0	7089	6680	348	308	21.7	1.1	Nd

Table 2
Carbon, oxygen, Sr isotopes and elemental composition of samples from the PS profile (Nd = not determined)

Sample	Lithology	Height (m)	$\delta^{13}C_{PDB}$	$\delta^{18}O_{PDB}$	Mg/Ca	Al (ppm)	Fe (ppm)	Mn (ppm)	Sr (ppm)	Fe/Sr	Mn/Sr	$^{87}Sr/^{86}Sr$
Cac-15 A	Limestone	5	−3.5	−9.5	22.3	2346	2396	228	443	5.4	0.5	Nd
Cac-16	Limestone	40	−2.7	−8.8	39.1	8515	4618	95	1335	3.5	0.1	0.70753
Cac-12 A	Limestone	80	Nd	Nd	35.4	2963	1379	52	1225	1.1	0.0	Nd
Cac-11	Limestone	95	−2.2	−7.7	41.5	4588	1931	39	1137	1.7	0.0	Nd
Cac-09	Limestone	135	−1.6	−8.1	25.6	1614	1024	39	1231	0.8	0.0	0.70754
Cac-08	Limestone	155	Nd	Nd	48.1	2056	1192	31	1146	1.0	0.0	Nd
Cac-06	Limestone	195	−1.4	−8.2	57.5	5338	2395	73	1228	1.9	0.1	0.70761
Cac-04	Limestone	210	−1.7	−10.6	92.5	4496	2174	49	434	5.0	0.1	Nd
Cac-02	Dolostone	216	−0.6	−5.8	660.9	762	635	71	35	18.1	2.0	Nd
Araras-30	Dolostone	220	−1.0	−0.8	619.2	837	718	36	57	12.6	0.6	Nd
Araras-29	Dolostone	240	Nd	Nd	624.0	1560	1214	41	46	26.4	0.9	Nd
Araras-28	Dolostone	280	Nd	Nd	616.4	2684	1099	65	57	15.3	1.1	Nd
Araras-27	Dolostone	320	+2.2	−0.1	605.3	3221	668	24	58	11.5	0.4	0.70982
Araras-26	Dolostone	360	Nd	Nd	554.2	4932	1966	46	65	30.2	0.7	Nd
Araras-23	Dolostone	480	+2.7	−1.6	611.0	183	159	7	31	5.1	0.2	0.70854
Araras-20	Dolostone	600	+1.9	−2.0	620.8	1358	444	12	59	7.5	0.2	0.70734
Araras-16	Dolostone	760	+1.9	−3.4	620.6	123	105	7	50	2.1	0.1	Nd
Araras-13	Dolostone	880	+2.7	−3.7	586.1	2179	327	20	97	3.4	0.2	0.70875
Araras-10	Dolostone	1000	+2.4	−3.9	644.5	2503	795	41	111	7.2	0.4	Nd
Araras-06 B	Dolostone	1020	+2.4	−3.1	637.4	126	183	12	59	3.1	0.2	Nd
Araras-04	Dolostone	1110	+1.8	−3.9	649.9	2885	738	39	73	10.1	0.5	0.70870
Araras-02	Dolostone	1180	+4.1	−3.5	628.1	4186	875	25	70	12.5	0.4	Nd
Araras-01 D	Dolostone	1225	+9.3	−1.9	622.8	3711	1037	50	50	20.7	1.0	Nd
Araras-01 C	Sand-dolostone	1227	Nd	Nd	648.0	13323	934	32	37	25.2	0.9	Nd
Araras-01 B	Dolostone	1237	+9.6	−3.2	656.8	6439	1110	53	49	22.6	1.1	0.70960
Araras-01 A	Sandstone		Nd	Nd	Nd	3917	285	5	5	5.7	0.1	Nd
Sítio	Dolostone	1320	+5.0	−0.9	556.9	Nd	Nd	Nd	Nd	Nd	Nd	Nd
Araras-31	Dolostone	1400	−1.0	−7.3	111.5	3441	1339	52	496	2.7	0.1	0.70907

Table 3
Carbon, oxygen, Sr isotopes and elemental composition of samples from the NSG profile (Nd = not determined)

Sample	Lithology	Height (m)	$\delta^{13}C_{PDB}$	$\delta^{18}O_{PDB}$	Mg/Ca	Al (ppm)	Fe (ppm)	Mn (ppm)	Sr (ppm)	Fe/Sr	Mn/Sr	$^{87}Sr/^{86}Sr$
Guia-01 A	Lime-shale	0	−5.3	−11.2	34.81	30582	11724	314	299	39.2	1.05	
Guia-01 B	Limestone	4	−3.8	−13.5	343.1	20220	10314	707	339	30.4	2.1	0.71219
Guia-02	Lime-shale	9	−2.0	−10.9	729.1	52346	15819	455	93	170.1	4.9	
Guia-04	Limestone	26	−3.6	−8.6		Nd	Nd	Nd	Nd	Nd	Nd	
Guia-05	Limestone	36	−2.1	−13.2	134.4	17600	5950	230	Nd	Nd	Nd	0.70964
Guia-06	Limestone	Nd	Nd	Nd	139.0	8077	2986	180	417	7.2	0.4	
Guia-07	Limestone	56	−0.9	−9.5	14.8	1229	828	65	1329	0.6	0.2	
Guia-10	Limestone	91	−1.5	−8.8	208.7	18021	9174	460	454	20.0	1.0	
Guia-13 A	Lime-shale	120	−0.8	−7.1	319.1	21330	10711	474	262	40.1	1.8	
Guia-13 C	Limestone	122	−1.0	−7.7	176.2	10120	4791	290	369	13.0	0.8	
Guia-15 A	Limestone	142	−1.4	−8.7	Nd	Nd	Nd	Nd	Nd	Nd	Nd	
Guia-16	Dolostone	147	−1.0	−7.7	506.6	5665	3470	182	258	13.4	0.7	
Guia-18	Dolostone	162	−1.5	−9.2	514.5	6401	3055	159	180	17.0	0.9	0.71151
Guia-20	Dolostone	171	+3.8	−10.1	Nd	Nd	Nd	Nd	Nd	Nd	Nd	
Guia-21	Lime-shale	180	+0.7	−14.9	186.3	30791	10053	774	318	31.6	2.4	

5.1. Mirassol d'Oeste (MDO)

This area consists of a lower dolostone and upper limestone sequence in which the $\delta^{13}C_{PDB}$ value range from −10.5 to −2.7‰ (Table 1, Fig. 6). The lower isotopic values are associated with the more intensely recrystallized and diagenetically affected samples, and by the presence of dissolution features (e.g., stylolites and voids). Because of these diagenetic features, we argue that these samples may have been affected by post-depositional processes, as indicated by the high Mn/Sr (>7.1) and Fe/Sr ratios, and thus do not record the primary isotopic signature. Limestone samples from the upper part of this sequence have low Mn/Sr (1.1) and present $\delta^{13}C$ values ranging from −4.6 to –2‰.

The oxygen isotopic composition of carbonate rock samples from this sequence range from −3.4 to −7.9‰ and do not show correlation with Mg/Ca and Mn/Sr ratios (Fig. 6, Table 1).

Three samples from the Mirassol d'Oeste section analyzed for $^{87}Sr/^{86}Sr$ ratios presented isotopic values ranging from 0.70803 to 0.70852. Two samples of dolostone have high Mn/Sr >7.3 ratios and $^{87}Sr/^{86}Sr$ ranging between 0.70848 and 0.70852, whereas the limestone sample present low Mn/Sr and Fe/Sr ratios and $^{87}Sr/^{86}Sr$ equal to 0.70803 (Table 1). The $^{87}Sr/^{86}Sr$ values obtained for this limestone, which also have high Sr content (412 ppm), is interpreted as reflecting the primary isotopic values.

5.2. Província Serrana (PS)

Among the three areas studied, the PS presents the most complete section including the whole carbonate sequence of the Araras Formation (Fig. 8). This section was sampled near Cáceres and Bauxi (Figs. 2 and 3, Table 2). The limestone samples in the lowermost Araras Formation are characterized by very high Sr concentration (434–1335 ppm), resulting in very low Mn/Sr (≤0.1) and Fe/Sr (≤3.5) ratios. The dolostone samples of the top of the Araras Formation have slightly elevated Mn/Sr (0.1–2.0) and Fe/Sr (2.1–30.2) ratios, which are probably related to dolomitization.

The $\delta^{13}C_{PDB}$ values for samples from the lower part of the PS section (Araras Formation) reveal that limestones overlying the diamictites present negative carbon isotope values that increase from the base to the top of the sequence (from −3.5 to −0.6‰). These low $\delta^{13}C_{PDB}$ values are found within the first 200 m of limestone and suggest that they were formed during post-glacial sea-level rise. The limestone grades within 3 m upwards to dolostones which are characterized by homogeneous and positive $\delta^{13}C_{PDB}$ values (+1.9 to +2.7‰). The upper part of the Araras Formation is formed by quartz- and feldspar-bearing sandy limestone presenting $\delta^{13}C_{PDB}$ values up to +9.6‰. The increase in the carbon isotopic values observed across 200 m of the profile, reveals that the deposition of these rocks occurred under contrasting environmental conditions. At the top of the Araras Formation, and just below the contact with the upper siliciclastic sequence, an abrupt decrease in $\delta^{13}C_{PDB}$ values is observed (down to −1.0‰).

The oxygen isotopic compositions across the profile range between −10.6 and −0.1‰, and depend on the dominant carbonate mineralogy. In the lower portion of the profile (calcite-bearing rocks) the $\delta^{18}O_{PDB}$ values range between −10.6 and −7.7‰, whereas in the upper portion of the profile (dolomite-bearing rocks) the $\delta^{18}O_{PDB}$ values range between −0.1 and −5.8‰ (Fig. 8, Table 2). Similarly, Sr concentration and isotopic ratio also vary according to the carbonate mineralogy. Limestone at the lower portion of the profile present low Mn/Sr ratios, high Sr concentrations, and a narrow range of $^{87}Sr/^{86}Sr$ ratio (from 0.70753 to 0.70761). In contrast, dolostone from the upper portion of the profile have low Mn/Sr ratios, but low Sr concentration and a wide range of $^{87}Sr/^{86}Sr$ ratios (from 0.70734 to 0.70982) (Table 2). Field evidence and petrographic observations suggest that the lower part of the carbonate sequence was deposited in a deep-water sub-wave condition, similarly to other coeval cap carbonates (Kennedy, 1996; James et al., 2001; Hoffman and Schrag, 2002). The data presented here, also indicate that these rocks preserve the primary $^{87}Sr/^{86}Sr$ isotopic composition of the seawater. In contrast, the dolostones may have been affected by post-depositional fluids during dolomitization.

5.3. Nossa Senhora da Guia syncline (NSG)

The NSG section (Fig. 11) is located in the inner part of the belt and was affected by low-grade metamorphic conditions. Rocks of the lower part of this section are exposed a few meters over the diamictite

and consist of low $\delta^{13}C_{PDB}$ laminated limestones and calc-shales. Similar to carbonate from the MDO and PS profiles, these rocks were probably deposited under the influence of post-glacial warming. Their negative carbon isotope values persist for 160 m above the lower contact and are not affected by facies variations, carbonate mineralogy (limestone-dolostone transitions) and rock texture. It is noteworthy however, that $\delta^{13}C_{PDB}$ values up to 4‰ were found in dolostones and calc-shale that occur within the last 20 m of the profile.

The oxygen isotope values of this profile vary between −14.9 and −7.2‰. Contrasting to the PS profile, there is no relationship between $\delta^{18}O_{PDB}$ and Mg/Ca ratio in these rocks, probably because they present a significant pelitic fraction and were disturbed by the low-grade metamorphism (Table 3).

Carbonate from the Guia sequence are intercalated with fine-grained siliciclastic sediments and were submitted to low grade metamorphic conditions. Their strontium isotopic ratios are significantly higher (between 0.70964 and 0.71219) than other carbonates investigated here, most likely due to metamorphism.

6. Correlations between the studied sections

All three sections described in this study initiate with carbonates directly overlying glacial diamictites. Since there is no available geochronological data for these rocks, an apparent age may be estimated based on the carbon and on the strontium isotopic composition of the carbonates. Strontium isotopes evolution curves for Neoproterozoic carbonates show that post Sturtian sediments present strontium ratios ranging between 0.7063 and 0.7074, whereas post Varangian/Marinoan carbonates present strontium ratios ranging between 0.7068 and 0.7087 (Kaufman et al., 1997; Jacobsen and Kaufman, 1999). Among the three profiles being studied here, the PS carbonates present the best preserved strontium isotopic ratios (between 0.70753 and 0.70761) based on their Mn/Sr and Fe/Sr ratios. These values indicate a Marinoan age for the glacial sediments of the Paraguay Belt. Both the MDO and the NSG carbonates present evidence of post-depositional disturbance of the strontium isotope ratios, which was related to dolomitization/re-crystallization and low-grade metamorphism, respectively.

The glacial unit underlying the carbonate rocks have been interpreted as representing a single glacial event, based mainly on its widespread and continuous distribution across the Paraguay Belt (Luz et al., 1978) (Fig. 2) (Rocha-Campos and Hasuí, 1981; de Alvarenga and Trompette, 1992; de Alvarenga et al., 2000).

Despite their different lithologic characteristics, the lower portion of these sequences present similar and comparable carbon isotopic values. The base of the PS and NSG sections is formed by limestone, whereas the base of the MDO section is made of dolostone which are overlain by laminated limestone. Hence, we argue that the first 200 m of the Araras Formation in the PS and NSG profiles can be correlated in terms of their lithological composition as well as of their carbon and oxygen isotope stratigraphy.

The lowest $\delta^{13}C_{PDB}$ values found in the MDO (−10.5 and −9.6‰) are related to dolostones overlying (first 22 m of section) the Puga Formation diamictite (Fig. 6). These low $\delta^{13}C_{PDB}$ values may be explained by post depositional processes, such as dolomitization (Fig. 7), that also imprinted higher Mn/Sr ratios in these rocks, precluding the chemostratigraphic correlation of MDO with other profiles. Over this horizon are ribbon limestones and laminated shales with $\delta^{13}C_{PDB}$ values ranging between −2.7 and −4.6‰ (Fig. 6), which can be correlated with the lower carbonate of PS and NSG sections.

The isotopic profiles of the three studied sections reveal similar negative $\delta^{13}C_{PDB}$ values (between −4.5 and −0.6‰) for laminated limestones and clay-limestones capping glacial intervals (Figs. 6, 8, and 12), representing, therefore, the deglaciation record of the Marinoan event. Available isotopic values suggest that this glacial record extends to the southern part of the Paraguay Belt where low $\delta^{13}C_{PDB}$ values (−5.4‰) for pinkish cap dolostone overlying the Puga Formation diamictites (Boggiani et al., 1997).

In contrast with the lower portion of the stratigraphic section, rocks from the upper portion of the Araras Formation has sedimentary structures typical of shallow carbonate platforms. The dolostones present uniform positive $\delta^{13}C_{PDB}$ values (+1.9 to +2.4‰)

across more than 800 m of the PS section (Fig. 8). These carbonates may correspond to the upper 70 m of the Tamengo Formation limestones which outcrop near Corumbá and in which *Cloudina* fossils have been found (Boggiani et al., 1997). The available isotope data of the Ediacaran fauna interval show slightly positive carbon isotope values worldwide (Lambert et al., 1987; Burns and Matter, 1993; Narbonne et al., 1994; Kaufman and Knoll, 1995).

The upper part of the PS section (Fig. 8) presents a well-defined positive $\delta^{13}C_{PDB}$ peak (+4.1 to +9.6‰), which has not been observed in the MDO and NSG sections.

7. Neoproterozoic Basins: a discussion

Two main distinct glaciogenic units covered by cap carbonates are present in Neoproterozoic sequences of Brazil. The older cap carbonate sequence covers large areas of the São Francisco Craton and of the surrounding Brasiliano belts. The cap carbonates are at the base of the Bambuí (Sete Lagoas Formation) and Una groups, which overly respectively glacial diamictites of the Jequitaí and Bebedouro formations (Dardenne, 1978; Misi and Veizer, 1998; Uhlein et al., 1999; Santos et al., 2000). Well-preserved and undeformed limestone samples from the Sete Lagoas Formation cap carbonate show a narrow range of Sr isotopic values (0.7074) and the Pb–Pb isochron age of 740 ± 22 Ma (Babinski and Kaufman, 2003) supporting that these glacial diamictites are, therefore, related to the "Sturtian" event.

The younger glaciogenic unit (Marinoan Age) is exposed in the Paraguay Belt and in the adjacent border of the Amazon Craton, being overlain by thick limestones and dolostones of the Araras Formation and Corumbá Group (Rocha-Campos and Hasuí, 1981; de Alvarenga and Trompette, 1992; Trompette et al., 1998; Nogueira et al., 2003). The age of this glaciation is estimated on the basis of microfossil assemblage found in post-glacial carbonate sequence that points to Vendian palaeoclimatic conditions in SW-Gondwana (Zaine and Fairchild, 1985; Gaucher et al., 2003). The strontium isotopic data presented in this paper, also support a Marinoan Age for the Paraguay Belt glaciation, and allow correlation, based on chemostratigraphy, with other Neoproterozoic cap carbonates basins.

Carbon isotopic profiles for carbonates of the Bambuí-Una Group and the Araras Formation are significantly different. Negative $\delta^{13}C_{PDB}$ values for the Araras and Guia carbonates occur across a 200 m thick sequence, whereas in the Bambuí Group negative $\delta^{13}C_{PDB}$ values are found only within a few meters of the base of the unit. Besides the difference observed in the lower part of the section, the Bambuí carbonate sequence exhibit an important and extensive positive $\delta^{13}C_{PDB}$ excursion (from +6.9 to +16.0‰) representing a chronostratigraphic marker within the entire basin (Martins, 1999; Santos et al., 2000). This pattern is not found in the Paraguay Belt, where most of the sequence (800 m thick) is characterized by a persistent low positive $\delta^{13}C_{PDB}$ values (from +1.9 to +2.4‰). Highly positive $\delta^{13}C_{PDB}$ values (+4.1 to +9.6‰) are observed only across a ∼100 m thick sequence (Fig. 8).

The low $\delta^{13}C_{PDB}$ values of carbonates rocks that cap the Marinoan and Sturtian glacial rocks are related to global sea level changes. The thick cap carbonate sequence of the Araras Formation was related to a deep water transgressive system, that was associated with the post-glacial sea level rise. The preservation of these thick sedimentary sequences suggest that a high-rate of tectonic subsidence was required to accommodate more than 200 m of sediments and warrant the isostatic adjustment related to the end of the glacial event. Our data also indicate possible correlation between the cap carbonates of the Araras Formation and other Neoproterozoic sections worldwide related to the Marinoan global glaciation event. Moreover, paleomagnetic data have indicated that glaciomarine diamictites of Puga Formation from Mirassol d'Oeste were deposited at low latitudes ("ice house") and that the cap carbonate are the result of an abrupt warming climate change ("greenhouse"), in agreement with the snowball hypothesis (Trindade et al., 2003).

In most cases, cap carbonates are characterized by 30–40 m thick layers of carbonates, thus contrasting with the 200 m thick cap carbonate found in the Paraguay Belt. Similar anomalous thick cap sequence have also been reported in Namibia, where more than 200 m of post-glacial carbonates (Buschmannsklippe Formation) with constant and negative $\delta^{13}C_{PDB}$ values have been identified (Kaufman et al., 1991; Kaufman and Knoll, 1995; Saylor et al., 1998; Fölling and Frimmel, 2002). Also in Namibia (southern Congo

Craton), carbon isotope data from the Maieberg cap-carbonate sequence, which overlies the glacial Ghaub Formation, are depleted in $\delta^{13}C_{PDB}$ for more than 300 m (Kaufman et al., 1991; Hoffman et al., 1998b; Kennedy et al., 1998; Hoffman and Schrag, 2002). The similarity between the carbon isotope profiles and $^{87}Sr/^{86}Sr$ ratios suggest that the section of the upper glacial intervals in the Otavi Platform (Ghaub Formation, southern Congo Craton) may be correlated with the cap carbonates of the Araras Formation. This correlation is possible if the Maiberg Formation overlies the Marinoan event (Kennedy et al., 1998; Hoffman and Schrag, 2002; Halverson et al., 2003), and not the Sturtian as suggested by others (Kaufman et al., 1997; Hoffman et al., 1998a,b).

The positive $\delta^{13}C$ excursions found in the upper part of the Araras Formation is marked by an abrupt change from deep-water deposition to shallow water dolostone platform facies. The $\delta^{13}C_{PDB}$ values within this interval varies from +1.9 to +2.7‰, and reach values as high as +9.6‰ at the top of the sequence. The high $\delta^{13}C_{PDB}$ values reported for the Araras Formation indicate the presence of very positive $\delta^{13}C$ values (>+8‰) in post Marinoan limestones deposits, reinforcing that the magnitude of the carbon isotope data constitute a poor criteria for distinguishing Sturtian from Marinoan glaciations (Kennedy et al., 1998).

8. Conclusions

The carbonate sequence of the Araras Formation (more than 1200 m) may be divided into four $\delta^{13}C$ chemo-stratigraphic intervals. A lower interval made of 22 m of cap dolomite with negative $\delta^{13}C_{PDB}$ values that overlie diamictite in the MDO area. These rocks were formed just after the end of the glacial period and are probably related to an abrupt environmental and seawater composition change. The second interval corresponds to the widespread cap carbonate occurrence of microcrystalline limestone intercalated with laminated mudstone. Rocks of this interval were identified in all three sections and present $\delta^{13}C_{PDB}$ values between −1.0 and −3.6‰. The third interval is marked by a narrow range of positive $\delta^{13}C$ values occurring across 800 m of dolostones that were deposited in a shallow and higher energy carbonate platform. The fourth interval is defined by a positive peak followed by an abrupt decrease in $\delta^{13}C_{PDB}$ value.

The thick carbonate layers with negative $\delta^{13}C_{PDB}$ deposited during the post-glacial transgressive event were interpreted as being formed in a deep shelf environment, allowing therefore the deposition of more than 200 m of limestone. These negative C-isotope value are common in other Neoproterozoic cap carbonates around the world and have been related to chemical oceanographic processes (Kaufman et al., 1997; Kennedy et al., 1998; Hoffman et al., 1998b; Hoffman and Schrag, 2002).

The data presented here show that the carbon isotope profiles across the Araras Formation carbonate sequence is significantly different from that of the Bambuí Group, another important Neoproterozoic sequence in central Brazil (Santos et al., 2000). In the Bambuí Group, negative $\delta^{13}C_{PDB}$ values are found only across a few meters of transgressive cap-carbonates that overly sturtian diamictites and are followed by a thick sequence of positive $\delta^{13}C_{PDB}$ carbonates (up to 13.5‰) (Misi and Kyle, 1994; Misi and Veizer, 1998; Santos et al., 2000).

The well-preserved $^{87}Sr/^{86}Sr$ isotopic ratios of cap carbonate samples of the Araras Formation range between 0.70753 and 0.70803 and together with the $\delta^{13}C_{PDB}$ values suggests a Marinoan age for the glacial event (Puga Formation).

Acknowledgements

This work was supported by “Programa de Ciência e Tecnologia do Petróleo (CTPETRO)” and “Conselho Nacional de Desenvolvimento Tecnológico (CNPQ)”. We are particularly grateful to M.M. Pimentel for his critical reading of the manuscript. Thanks are also given to A.J. Kaufman for his critical comments which improved significantly the manuscript.

References

de Almeida, F.F.M., 1964a. Geologia do centro-oeste matogrossense. Brazil Minist. Minas Energ. Dep. Nac. Prod. Miner. Bol. Div. Geol. Mineral 215, 1–137.

de Almeida, F.F.M., 1964b. Glaciação Eocambriana em Mato Grosso. Brazil Minist. Minas Energ. Dep. Nac. Prod. Mineral Notas Prelim. Est. 117, 1–10.

de Almeida, F.F.M., Mantovani, M.S.M., 1975. Geologia e geocronologia do granito de São Vicente, Mato Grosso. An. Acad. Bras. Ciênc. 47, 451–458.

de Alvarenga, C.J.S., 1990. Phénomènes sédimentaires, structuraux et circulation de fluides développés à la transition chaîne-craton. Exemple de la chaîne Paraguai d'âge protérozoïque supérieur, Mato Grosso, Brésil. Thesis doct. Univ. Aix-Marseille III, France, 177 pp. (unpublished).

de Alvarenga, C.J.S., Saes, G.S., 1992. Stratigraphy and sedimentology of the middle and late Proterozoic in the southeast of the Amazonian Craton. Rev. Bras. Geociênc. 22, 493–499.

de Alvarenga, C.J.S., Trompette, R., 1992. Glacial influenced turbidite sedimentation in the uppermost Proterozoic and Lower Cambrian of the Paraguay Belt (Mato Grosso, Brazil). Palaeogeogr. Palaeoclimatol. Palaeoecol. 92, 85–105.

de Alvarenga, C.J.S., Trompette, R., 1993. Brasiliano tectonic of the Paraguay Belt: the structural development of the Cuiabá Region. Rev. Bras. Geociênc. 23, 18–30.

de Alvarenga, C.J.S., Moura, C.A.V, Gorayeb, P.S.S., de Abreu, F.A.M., 2000. Paraguay and Araguaia Belts. In: Cordani, U.G., Milani, E.J., Thomaz Filho, A., Campos, D.A. (Eds.), Tectonic Evolution of South America. 31st International Geological Congress, Rio de Janeiro, pp. 183–193.

Asmeron, Y., Jacobsen, S.B., Knoll, A.H., Butterfield, N.J., Swett, K., 1991. Strontium isotopic variations of Neoproterozoic seawater: implications for crustal evolution. Geochem. Cosmochim. Acta 55, 2883–2894.

Babinski, M., Kaufman, A.J., 2003. First direct dating of a Neoproterozoic post-glacial cap carbonate. In: Proceedings of the IV South-American Symposium on Isotope Geology. Short Paper, Salvador, Brazil, pp. 321–323.

Barros, A.M., Silva, R.M., Cardoso, O.R.F.A., Freire, F.A., de Souza Jr., J.J., Rivetti, M., Luz, D.S. da, Palmeira, R.C.B., Tasinari, C.C.G., 1982. Folha SD21 Cuiabá, Geologia. In: RADAMBRASIL, vol. 26. Levant. Rec. Naturais, Rio de Janeiro, pp. 25–192.

Boggiani, P.C., Sial, A.N., Coimbra, A.M., Ferreira, V.P., 1997. The carbon and oxygen isotope record of Neoproterozoic carbonate rocks of the Paraguay fold belt (central South America). In: Proceedings of the South American Symposium on Isotope Geology, vol. 1, Extended Abstracts. Campos do Jordão, Brazil, pp. 57–59.

Bonhomme, M.G., Cordani, U.G., Kawashita, K., Macedo, M.H.F., Thomaz Filho, A., 1982. Radiochronological age and correlation of Proterozoic sediments in Brazil. Precambrian Res. 18, 103–118.

Brasier, M., McCarron, G., Tucker, R., Leather, J., Allen, P., Shields, G., 2000. New U–Pb zircon dates for the Neoproterozoic Ghubrah glaciation and for the top of the Huqf Supergroup. Oman Geol. 28, 175–178.

Burns, S.J., Matter, A., 1993. Carbon isotopic record of the latest Proterozoic from Oman. Eclogae Geol. Helv. 86, 595–607.

Chang, H.K., Kawashita, K., Alkmim, F.F., Moreira, M.Z., 1993. Considerações sobre a estratigrafia isótopica do Grupo Bambuí. In: Simpósio Sobre o Cráton do São Francisco, vol. 2. Anais, Salvador, Brazil, pp. 195–196.

Condon, D.J., Prave, A.R., 2000. Two from Donegal: Neoproterozoic glacial episodes on the northeast margin of Laurentia. Geology 28, 951–954.

Cordani, U.G., Thomaz Filho, A., de Brito Neves, B.B., Kawashita, K., 1985. On the applicability of the Rb–Sr method to argillaceous sedimentary rocks: some examples from Precambrian sequences of Brazil. J. Geol. 471, 253–280.

Dardenne, M.A., 1978. Síntese sobre a estratigrafia do Grupo Bambuí no Brasil Central. In: Congresso Brasileiro de Geologia, 30, Anais, Recife, Brazil, SBG, vol. 2. pp. 597–610.

Derry, L.A., Keto, L.S., Jacobsen, S.B., Knoll, A.H., Swett, K., 1989. Sr isotope variations in Upper Proterozoic carbonates from Svalbard and East Greenland. Geochim. Cosmochim. Acta 53, 2331–2339.

Fölling, P.G., Frimmel, H.E., 2002. Chemostratigraphic correlation of carbonate successions in the Gariep and Saldania Belts, Namibia and South Africa. Basin Res. 14, 69–88.

Gaucher, C., Boggiani, P.C., Sprechmann, P., Sial, A.N., Fairchild, T., 2003. Integrated correlation of the Vendian to Cambrian Arroyo del Soldado and Corumbá Groups (Uruguay and Brazil): palaeogeographic, palaeoclimatic and palaeobiologic implications. Precambrian Res. 120, 241–278.

Hahn, G., Hahn, R., Leonardos, O.H., Pflug, H.D., Walde, D.H.G., 1982. Körperlich erhaltene Scyphozoen—Reste aus dem Jungprakambrium Brasiliens. Geol. Palaeontol. 16, 1–18.

Halverson, G.P., Hoffman, P.F., Maloof, A.C., Rice, A.H.N., 2003. Towards a composite carbon isotope section for the Neoproterozoic. In: Proceedings of the IV South-American Symposium on Isotope Geology. Short Paper, Salvador, Brazil, pp. 14–17.

Hoffman, P.F., Schrag, D.P., 2002. The snowball Earth Hypothesis: testing the limits of global change. Terra Nova 14, 129–155.

Hoffman, P.F., Kaufman, A.J., Halverson, G.P., 1998a. Comings and goings of global glaciations on a Neoproterozoic tropical platform in Namibia. GSA Today 8, 1–9.

Hoffman, P.F., Kaufman, A.J., Halverson, G.P., Schrag, D.P., 1998b. A Neoproterozoic snowball earth. Science 281, 1342–1346.

Hyde, W.T., Crowley, T.J., Baum, S.K., Peltier, W.R., 2000. Neoproterozoic 'snowball Earth' simulations with a coupled climate/ice-sheet model. Nature 405 (6785), 425–429.

Iyer, S.S., Babinski, M., Krouse, H.R., Chemale Jr., F., 1995. Highly (super 13) C-enriched carbonate and organic matter in the Neoproterozoic sediments of the Bambuí Group, Brazil. Precambrian Res. 73, 271–282.

Jacobsen, S.B., 2001. Gas hydrates and deglaciations. Nature 412, 691–693.

Jacobsen, S.B., Kaufman, A.J., 1999. The Sr, C and O isotope evolution of Neoproterozoic seawater. Chem. Geol. 161, 37–57.

James, N.P., Narbonne, G.M., Kyser, T.K., 2001. Late Neoproterozoic cap carbonate: Mackenzie Mountains, northwestern Canada: precipitation and global glacial meltdown. Can. J. Earth Sci. 38, 1229–1262.

Karfunkel, J., Hoppe, A., 1988. Late proterozoic glaciation in central-eastern Brazil: synthesis and model. Palaeogeogr. Palaeoclimatol. Palaeoecol. 65, 1–21.

Kaufman, A.J., Knoll, A.H., 1995. Neoproterozoic variations in the C-isotope composition of seawater: stratigraphic and biogeochemical implications. Precambrian Res. 73, 27–49.

Kaufman, A.J., Hayes, J.M., Knoll, A.H., Germs, G.J.B., 1991. Isotopic compositions of carbonates and organic carbon from upper Proterozoic successions in Namibia: stratigraphic variation and the effects of diagenesis and metamorphism. Precambrian Res. 49, 301–327.

Kaufman, A.J., Jacobsen, S.B., Knoll, A.H., 1993. The Vendian record of Sr and C isotope variations in seawater: implications for tectonics and paleoclimate. Earth Planet. Sci. Lett. 120, 409–430.

Kaufman, A.J., Knoll, A.H., Narbonne, G.M., 1997. Isotopes, ice ages, and terminal Proterozoic earth history. Proc. Natl. Acad. Sci. U.S.A. 94, 6600–6605.

Kennedy, M.J., 1996. Stratigraphy, sedimentology, and isotopic geochemistry of Australian Neoproterozoic postglacial cap dolostone: deglaciation, $\delta^{13}C$ excursion, and carbonate precipitation. J. Sediment. Res. 66, 1050–1064.

Kennedy, M.J., Runnegar, B., Prave, A.R., Hoffmann, K.-H., Arthur, M.A., 1998. Two or four Neoproterozoic glaciations? Geology 26, 1059–1063.

Kennedy, M.J., Christie-Blick, N., Sohl, L.E., 2001. Are Proterozoic cap carbonates and isotopic excursions a record of gas hydrate destabilization following Earth's coldest intervals? Geology 29, 443–446.

Knoll, A.H., Grotzinger, J.P., Kaufman, A.J., Kolozov, P., 1995. Integrated approaches to terminal Proterozoic stratigraphy: an example from the Olenek Uplift, northeastern Siberia. Precambrian Res. 73, 251–270.

Lambert, I.B., Walter, M.R., Zang, W., Lu, S., Ma, G., 1987. Paleoenvironment and carbon isotope stratigraphy of upper Proterozoic carbonates of the Yangtze Platform. Nature 325, 140–142.

Litherland, M., Annels, R.N., Appleton, J.D., Berrangé, J.P., Bloomfield, K., Burton, C.C.J., Darbyshire, D.P.F., Fletcher, C.J.N., Hawkins, M.P., Klinck, B.A., Llanos, A., Mitchell, W.I., O'Connor, E.A., Pitfield, P.E.J., Power, G., Webb, B.C., 1986. The geology and mineral resources of the Bolivian Precambrian shields. Br. Geol. Surv. Overseas Mem. 9, 153.

Luz, J.S., Abreu Filho, W., 1978. Aspectos geológico-econômico da Formação Araras do Grupo Alto Paraguai—MT. An. 30°. Congr. Bras. Geol. Soc. Bras. Geol. Recife 4, 1816–1826.

Luz, J.S., Oliveira, A.M., Lemos, D.B., Argolo, J.L., Souza, N.B., Abreu, W., 1978. Relatório Final do Projeto Província Serrana (map). Dep. Nac. Prod. Mineral/Comp. Pesq. Rec. Minerais, Goiânia, 105 pp.

Maciel, P., 1959. Tilito Cambriano (?) no Estado de Mato Grosso. Soc. Brás. Geol. Boletim 8, 3–49.

Martins, M., 1999. Análise estratigráfica das seqüências mesoproterozóicas (borda oeste e neoproterozóicas da Bacia do São Francisco). Máster Universidade Federal do Rio Grande do Sul, Porto Alegre, Brazil, 214 pp.

McCrea, J.M., 1950. On the isotopic chemistry of carbonates and a paleotemperature scale. J. Chem. Phys. 18, 849–857.

Misi, A., Kyle, J.R., 1994. Upper Proterozoic carbonate stratigraphy, diagenesis, and stromatolitic phosphorite formation, Irecê Basin, Bahia, Brazil. J. Sediment. Res. A64, 299–310.

Misi, A., Veizer, J., 1998. Neoproterozoic carbonate sequence of the Una Group, Irecê Basin: chemostratigraphy, age and correlations. Precambrian Res. 89, 87–100.

Myrow, P.M., Kaufman, A.J., 1999. A newly discovered cap carbonate above Varanger-Age glacial deposits in Newfoundland, Canada. J. Sediment. Res. 69, 784–793.

Narbonne, G.M., Kaufmann, A.J., Knoll, A.H., 1994. Integrated chemostratigraphy and biostratigraphy of the upper Windermere Supergroup (Neoproterozoic), Mackenzie Mountains, northwestern Canada. Geol. Soc. Am. Bull. 106, 1281–1291.

Nogueira, A.C.R., Riccomini, C., Sial, A.N., Moura, C.A.V., Fairchild, T.R., 2003. Soft-sediment deformation at the base of the Neoproterozoic Puga cap carbonate (southwestern Amazon craton, Brazil): confirmation of rapid icehouse to greenhouse transition in snowball Earth. Geology 31, 613–616.

Pimentel, M.M., Fuck, R.A., de Alvarenga, C.J.S., 1996. Post-Brasiliano (Pan-African) high-K granitic magmatism in central Brazil: the role of late Precambrian-early Paleozoic extension. Precambrian Res. 80, 217–238.

Rocha-Campos, A.C., Hasuí, Y., 1981. Late Precambrian Jangada Group and Puga Formation of Central Western Brazil. In: Hambrey, M.J., Harland, W.B. (Eds.), Earth's Pre-Pleistocene Glacial Record. Cambridge University Press, pp. 916–919.

Santos, R.V., de Alvarenga, C.J.S., Dardenne, M.A., Sial, A.N., Ferreira, V.P., 2000. Carbon and oxygen isotope profiles across Meso-Neoproterozoic limestones from central Brazil: Bambuí and Paranoá groups. Precambrian Res. 104, 107–122.

Saylor, B.Z., Kaufman, A.J., Grotzinger, J.P., Urban, F., 1998. A composite reference section for terminal Proterozoic strata of southern Namibia. J. Sediment. Res. 68, 1223–1235.

Schimidt, W.P., Williams, E.G., Emblenton, J.J.B., 1991. Low paleolatitude of Late Proterozoic glaciation: early timing of remanence in haematite of the Elatina formation, South Australia. Earth Planet. Sci. Lett. 105, 355–367.

Scobbenhaus, C., Campos, D.A., Derze, G.R., Asmus, H.E., 1981. Mapageológico do Brasil e da área oceânica adjacente incluindo depósitos minerais. Escala 1/2.500.000. Dep. Nac. Produç. Mineral (DNPM), Brasíia.

Toulkerids, T., Babinski, M., Buchwaldt, R., de Brito Neves, B.B., Todt, W., Santos, R.V., 1999. Are Varangian or Sturtian the glacial deposits on the São Francisco Craton? Evidence from age determination of sedimentary rocks and mineral of the neoproterozoic Una Group. In: Proceedings of the South-American Symposium on Isotope Geology, vol. 2. Actas, Cordoba, Argentina, pp. 453–456.

Trindade, R.I.F., Fonta, E., D'Agrella-Filho, M.S., Nogueira, A.C.R., Riccomini, C., 2003. Low-latitude and multiple geomagnetic reversals in the Neoproterozoic Puga cap carbonate of Amazonia. Terra Nova, p. 15.

Trompette, R., 1994. Geology of Western Gondwana (2000–500 Ma). Pan-African—Brasiliano Aggregation of South America and Africa. Balkema, 350 pp.

Trompette, R., 1996. Temporal relationship between cratonization and glaciation: the Vendian-early Cambrian glaciation in Western Gondwana. Palaeogeogr. Palaeoclimatol. Palaeoecol. 123, 373–383.

Trompette, R., 1997. Neoproterozoic (~600 Ma) aggregation of Western Gondwana: a tentative scenario. Precambrian Res. 82, 101–112.

Trompette, R., de Alvarenga, C.J.S., Walde, D., 1998. Geological evolution of the Neoproterozoic Corumbá graben system (Brazil). Depositional context of the stratified Fe and Mn ores of Jacadigo Group. J. South Am. Earth Sci. 11, 587–597.

Uhlein, A., Trompette, R., de Alvarenga, C.J.S., 1999. Neoproterozoic glacial and gravitational sedimentation on a continental rifted margin: the Jequitaí—Macaúbas sequence (Minas Gerais, Brazil). J. South Am. Earth Sci. 12, 435–451.

Walde, D.H.G., Leonardos, O.H., Hahn, G., Pflug, H.D., 1982. The first pre-Cambrian megafossils from South America, *Corumbella werneri*. An. Acad. Bras. Ciênc. 54, 461.

Walter, M.R., Veevers, J.J., Calver, C.R., Gorjan, P., Hill, A.C., 2000. Dating the 840–544 Ma Neoproterozoic interval by isotope of strontium, carbon, and sulfur in seawater, and some interpretative models. Precambrian Res. 100, 371–433.

Young, G.M., 1995. Are Neoproterozoic glacial deposits preserved on the margins of Laurentia related to the fragmentation of two supercontinents? Geology 23, 153–156.

Zaine, M.F., 1991. Análise dos fósseis de parte da faixa Paraguai (MS, MT) e seu contexto temporal e paleoambiental. Thesis dout. Univ. São Paulo, Brasil, Inst. Geocienc., 215 pp. (unpublished).

Zaine, M.F., Fairchild, T.R., 1985. Comparaison of Aulophycus Lucianoi BEURLEN and Sommer from Ladário (MS) and the genus Cloudina Germs, Ediacaran of Namibia. An. Acad. Brasileira Ciênc. Rio de Janeiro 57, 180.

Zaine, M.F., Fairchild, T.R., 1987. Novas considerações sobre os fósseis da formação Tamengo, grupo Corumbá, SW do Brasil. An. X° Congr. Brasil. Paleont., Rio de Janeiro, Tamengo, grupo Corumbá, SW do Brasil. An. X° Congr. Brasil. Paleont., Rio de Janeiro, Brazil, pp. 797–806.